CONTROL STRATEGY AND FLOW SIMULATION OF AN ONDULATORY BLADE PUMP FOR BIOMEDICAL PURPOSES

Flávio J. A. Soares, acadaf@usp.br
Raul G. Lima,
Mechanical Engineering Department, Escola Politécnica, USP

Abstract.*This work presents a design methodology for oscillating blade pumps using numerical simulations. The aim is to design a pump with low frequency and efficient. The blade performs a propagating transversal wave. Contact between the blade and the pump case is avoided and the velocity between blade and pump case should be low. A numerical simulation tool is required since an analytical solution is not feasible. The Finite Elements Method is used to solve the Navier-Stokes equations and the blade movement is represented through moving boundaries. A search algorithm is employed to determine inflow velocity. Numerical simulations were performed. The efficiency and pressure head were computed for twenty sets of design parameters. Twelve electromagnetic actuators and five differential capacitors had been built to control the blade movement. Amplitude of oscillations and frequency of oscillations are design variables. A map from design variables to efficiency and head pressure was computed.*

Keywords: *hemolysis, oscillating blade, fluid dynamics, pump...*

1. INTRODUCTION

The aim of this work is to develop a design tool for a pump with low frequency of *ondulatory* movements of a single oscillating blade. Several authors are developing oscillating blade pumps, Laser (2003), Triantafyllou (1996), Triantafyllou (1995), Gopalkrishnam (1994). Through a deep analysis of fish movements the principles of oscillating blade propulsion were explained and used in pumps. On one side, there are oscillating pumps which mimic ostraciiform fishes and the movement of the blade is called *oscillatory*, Nakasone (2005). On the other extreme, there are pumps that mimic anguilliform fishes and the movement of the blade is called *ondulatory*. The design tool developed in this work is concerned with ondulatory movement of the blade, which is expected to generate lower hemolysis rate in a biological context.

The numerical simulation of the flow through the pump gives the field of velocity and the pressure field. The velocity and pressure fields are used to compute the efficiency of a particular pump design. Once the efficiency can be computed, a procedure to find an optimal set of design parameters can be implemented.

1.1 Moving Boundaries

It is necessary to solve Navier-Stokes equations imposing the movement of the blade. This is accomplished using the concept of moving boundaries. Moving boundaries can be implemented with or without mesh deformation, Turek (1998). The implementation of moving boundaries is accomplished without mesh deformation and this region is called artificial moving boundaries. The fluid has null normal velocity relative to the moving boundary. The moving boundary corresponds to a region that moves inside of a fixed domain, it imposes restrictions to the velocity field.

1.2 Control Volume

The domain represents a duct of square transversal shape. On one extremity the blade is hinged. On the other extremity the blade is simply supported. The imposed boundary conditions are the outlet surface mean pressure, the inlet surface velocity distribution, blade shape, blade amplitude and blade movement frequency. The flow of an incompressible fluid is represented by the Navier-Stokes equation (1) and the continuity equation (2),

$$\vec{u}_t - \nu\Delta\vec{u} + \vec{u}\nabla\vec{u} + \nabla p = \vec{f} \tag{1}$$

$$\nabla\vec{u} = 0 \tag{2}$$

where p is the normalized pressure, namely, pressure divided by density, see equation (3), ρ is the density, u is the velocity vector, and f is the vector of field external forces.

$$p = \frac{P}{\rho} \tag{3}$$

1.3 Blade Movement

The blade movement is given by equation (4), which is a propagating sinusoidal wave, attenuated at the extremities by equation (5). The product of these two equations is called as blade wave equation (6).

$$A \sin\left(\frac{\pi}{a}(x - x_0) - \phi\Delta t\right) \tag{4}$$

$$[1 - e^{-(x-x_0)}][(1 - exp^{(x-x_0)-cv}] \tag{5}$$

$$y(x,t) = y_0 + A\left(1 - e^{-(x-x_0)}\right)\left(1 - exp^{(x-x_0)-20}\right)\sin\left[\frac{\pi}{a}(x - x_0) - \phi t\right] \tag{6}$$

where x_0 and y_0 are the coordinates of the origin of the blade, x and y are the coordinates of a point of the blade, cv is the blade length, ϕ is the angular velocity and t is time.

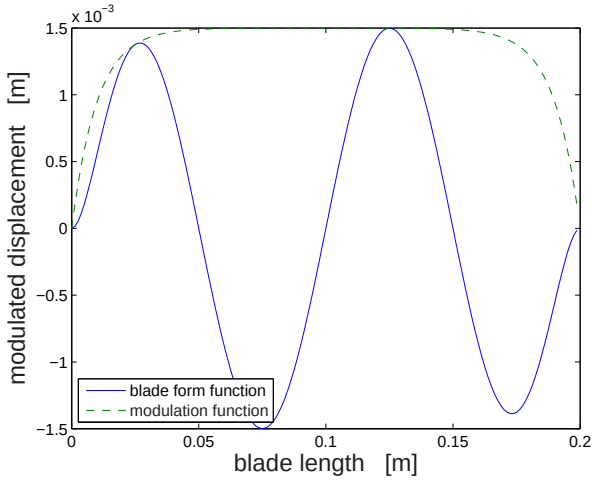

Figure 1. Blade wave equation.

2. Methodology

The basic tools to search for the optimal design parameters are a *numerical pump*, which is an algorithm for the determination of velocity and pressure fields, a *performance index*, which is the mechanical efficiency of the pump in the present work but can be extended to incorporate the hemolysis rate in a future work. An *experimental pump* is under development to evaluate the performance of the numerical pump. In the following paragraphs the status of these three basic elements are described.

2.1 Experimental Pump

The dimensions of the experimental pump are the same as dimensions of the numerical pump. The adopted fluid in this work is water and, therefore, the kinematic viscosity is $0,993e^{-6}\ m/s$ at 20^oC.

To control the blade shape, 12 electromagnetic actuators were developed and it should work as shown on Figure (2), which represents only one side of the pump. The blade is made of ferromagnetic 0.02 mm thickness stainless steel.

The current intensity on each actuator is determined by feedback control, given the blade movement. Equation (6) determine the target displacement history on each actuator.

The non linear characteristics of the electromagnetic actuators must be taken into account. The control strategy is a MIMO state-space pole allocation algorithm.

2.1.1 Electromagnetic Actuators

The electromagnetic actuator have a core made of silicon iron blades with oriented grains overlapped with Epoxy layers. The force induced by one solenoid is given by equation (7), Boffi (1977), which represents a non linear relationship between force f and current i, as well as, a non linear relationship between force and distance y.

$$f_{mag} = \mu_0^2 \frac{n_e^2 i^2}{4} \frac{l^2}{y^2} \tag{7}$$

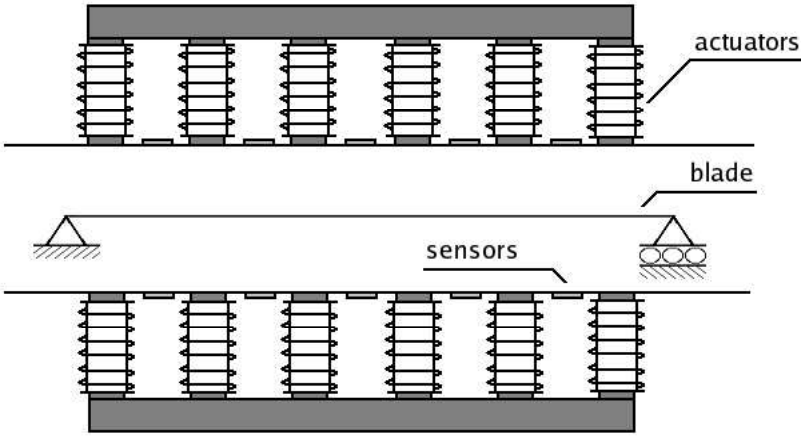

Figure 2. Schematics of electromagnets acting on the blade

where n is the number of turns of the solenoid, μ_0 is the electromagnetic permeability of air, l is the width of the solenoid and d is the length of the solenoid.

$$f_{mag} = \mu_{bomba}^2 \frac{n_e^2 i^2}{4} \frac{l^2}{y^2} \tag{8}$$

The electromagnetic attraction force over a blade region was experimentally determined, as shown in Figure (3).

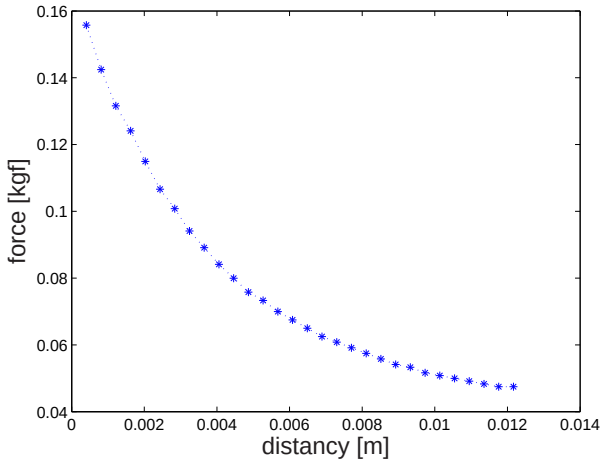

Figure 3. Electromagnetic attraction force over a blade region. Note the hyperbolic behavior of the force.

Having determined experimentally the electromagnetic attraction force, it was estimated the average electromagnetic permeability of aluminum, water and electromagnet core, see Figure (4).

2.2 Displacement Sensors

Differential capacitive sensors were built to serve as displacement sensors. One plate of the capacitor is a gold covered cupper square electrode of $1cm^2$, attached to the pump case inner wall and electrically isolated of the pump case. The other plate of the capacitor is the blade itself. The electric potential is measured between the cupper electrodes and blade, as shown in Figure (5). The fluid is the dielectric element. When the blade moves, the gap on each capacitive sensor changes.

According to Webster (1999), the capacitance is governed by the equation (9),

$$C = C(s, x, \mu) \tag{9}$$

$$C(x) = \frac{\mu s}{x} = \frac{\mu_r \mu_0 s}{x} \tag{10}$$

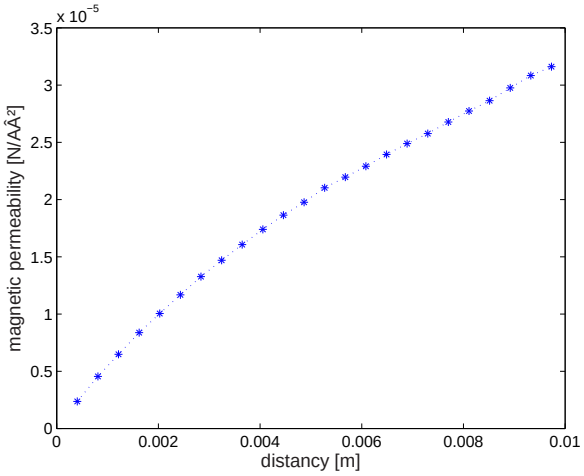

Figure 4. Effective electromagnetic permeability of aluminum, water and electromagnet core.

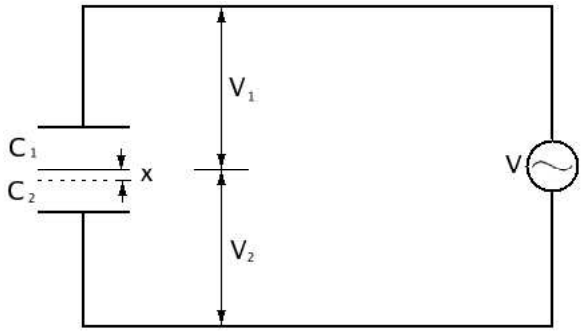

Figure 5. Differential capacitive displacement sensor.

where s is the area of the plates, $\vec{x}$ is the distance between the plates, μ is the magnetic permeability of the work fluid, μ_r is relative the magnetic permeability and μ_0 is the dielectric constant of the vacuum. The variation of the capacitance throughout the distance x becomes

$$\frac{dC}{dx} = -\frac{\mu_r \mu_0 s}{x^2} \tag{11}$$

Therefore, the sensitivity of the sensor is inversely proportional to the square power of the distance between the electrodes.

2.3 The Numerical Pump

The Finite Elements solver, Featflow-1.3RC3 (2005), is capable of imposing artificial moving boundaries and uses a multi-grid strategy to search for the solution of the Navier-Stokes equations. The multi-grid strategy gives robustness and speed for the computation. Typically the more refined mesh has 6 thousands nodes. The elements used were quadrilateral elements with piecewise rotated bilinear shape functions for velocities and piecewise constant pressure approximations.

The initial input velocity profile is a required initial boundary condition to solve Navier-Stokes equations through Featflow. A simple iterative algorithm was made to impose this initial condition. The average initial input velocity was taken as the smaller average velocity that gives positive pressure head.

2.4 Performance Index

The power efficiency was computed considering the power given by the pump divided by the power given to the pump. Three terms are evaluated, the power given to the pump by the inlet surface P_{in}, the power given to the pump through the blade displacement P_{fm} and the power given by the pump through the outlet surface P_{out}, see equation (12).

$$\eta = \frac{P_{out}}{P_{in} + P_{fm}} \tag{12}$$

The term P_{fm} is the integral of the work done by each element of the blade. The displacement of each element of the blade is computed by equation (6) and a certain time interval Δt. The resulting force on each element of the blade is evaluated using Newton's second law, which implies taking into account pressure on both sides of the blade, shear forces, and inertial forces.

The term P_{in} is the integral of the work done by each fluid element on the inlet surface. The displacement of each element is computed as velocity times the time interval Δt. The external force acting on each fluid element is evaluated as pressure times element area. The work done is the product of external force on each fluid element times the displacement. The pressure and velocity fields are given by the solution of Navier-Stokes equations.

The term P_{out} is the integral of the work done by each fluid element on the outlet surface. The displacement of each element is computed by velocity times the time interval Δt. The external force acting on each fluid element is evaluated as pressure times element area. The work done is the product of external force on each fluid element times the displacement. The pressure and velocity fields are given by the solution of Navier-Stokes equations.

2.5 Dynamic Blade Control

A FEM structural model was used to represent the blade with six beam elements. The number of elements was chosen such that each node lies in the position where an electromagnetic force is applied. On the same nodes displacements are measured. The control algorithm limits the transversal displacements in y direction. The longitudinal displacements, in x direction, are neglected. The shortening of the blade is not considered in the structural model of the blade. Taking into account actuators and sensors, the system state is controllable and observable. Therefore a pole allocation linear control strategy can be implemented

2.6 Numerical Results

Twenty sets of design parameters were numerically simulated, according to table 1. Each simulation required 4 hours on a Pentium 4, 2.2 GHz. The performance behavior, of some simulation is shown on Figure (6). Observe the pulsatile characteristic of the pump with the chosen parameters. Note also that when the frequency is doubled, the number of pulses per second is doubled.

Table 1. Sets of design parameters

Freq. [Hz]	Amplit. [cm]	Ang. Speed. [rad/s]	Wave Length [cm]
1	0.10	π	12
5	0.15	10π	12
10	0.20	20π	12
15	0.25	30π	12
20	-	-	-

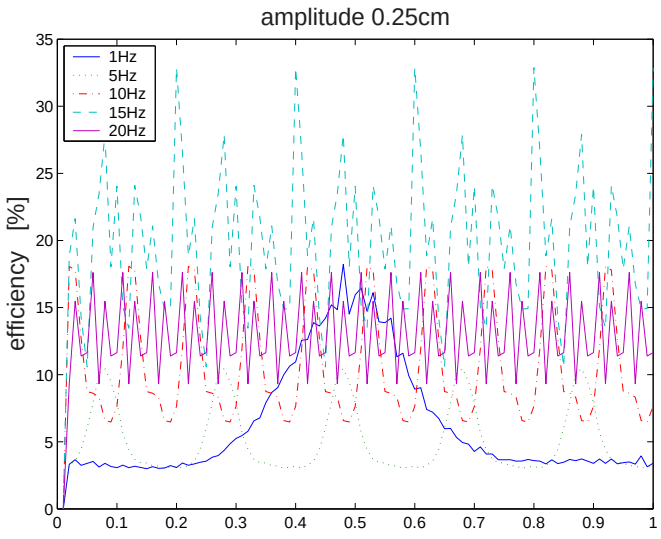

Figure 6. Power efficiency vs. oscillating frequencies.

Results of efficiency versus frequencies for several amplitudes are shown in Figure (7). Results of pressure head versus frequencies for several amplitudes are shown in Figure (8).

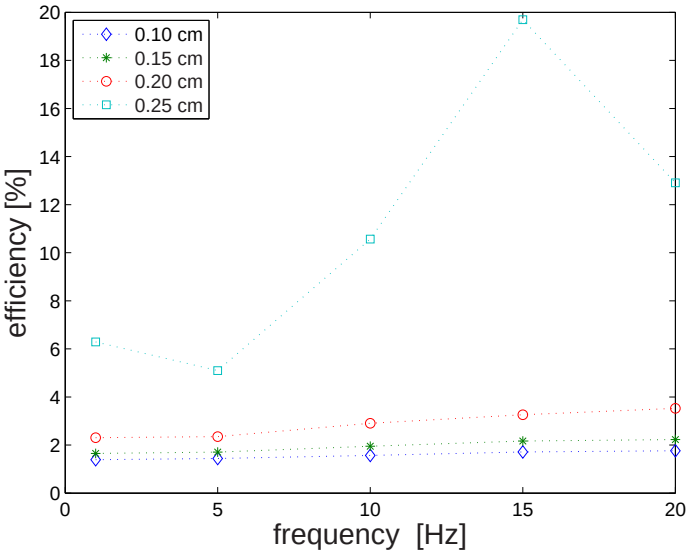

Figure 7. Efficiency vs. frequencies for several amplitudes.

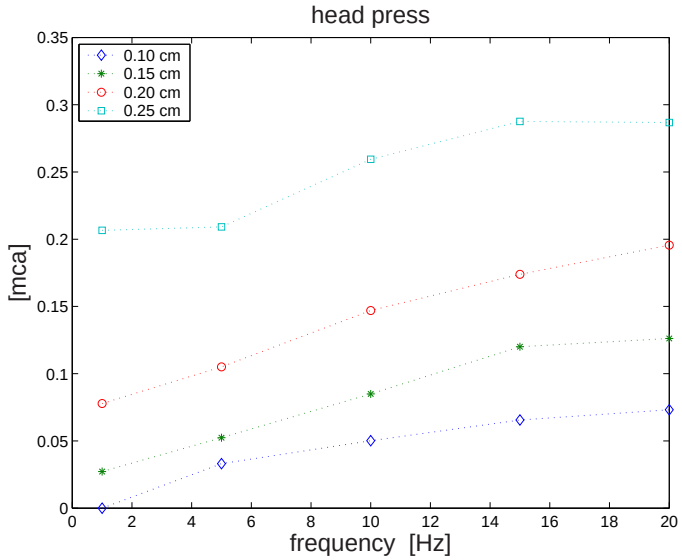

Figure 8. Pressure head vs. frequency for several amplitudes.

3. Final Comments

A design methodology for ondulatory blade pumps was developed including a numerical simulation methodology to compute the mechanical power efficiency, an algorithm to determine the inflow velocity and a map from design parameters to efficiency and pressure head. An experimental ondulatory pump is being assembled using the results of the numerical simulations presented. The experimental pump will be used to compare numerical results and measurements of pressure heads and flow.

4. Acknowledgments

The authors gratefully acknowledge the financial support given by Federal Center of Technological Education, CEFET-AM, and by State of the Amazon Research Foundation, FAPEAM, Ph.D. scholarship.

Boffi, L, V., Júnior M. S., Dangelo J. C. "Conversão Eletromecânica de Energia. Editora Edgar Blücher". 1977.
http://www.featflow.de/dosws/dfwin.html

Gopalkrishnam, R., Triantafyllou, Michael, S., Triantafyllou, George, S., and Barrett, D. S. "Active Vorticity Control in a Shear Flow Using a Flapping Foil". Journal of Fluid Mechanics. vol 274, pg 1-21.

Laser, D. J. e Santiago J. G. A Review of Micropumps. "Journal of Micromechanics and Microenginnering". 2003. Pgs. R35 - R64.

Nakasone, P. H., Cunha, M. R.,Andrade, A. J. P and Lima, C. R., Silva, E. C. N. "Mechatronic Pump Characterization: The $Mech_Pump$". Proceedings of 18th Congress of Mechanical Engineering COBEM, Ouro Preto, MG, November 6-11 2005.

Triantafyllou, Michael, S. and Triantafyllou, George, S. "An Efficient Swimming Machine. Scientific American",pg 40-48. March 1995.

Triantafyllou, Michael, S. and Triantafyllou, George, S. "A New Paradigm of Propulsion and Maneuvering for Marine Vehicles". SNAME Transactions. Vol. 104, pg 81-100ss. 1996.

Turek, S. "Efficient Solvers for Incompressible Flow Problems - An Algorithmic Approach in View of Computational Aspects", pp 12. Springer. Heidelberg, October 1998.

Webster, J. G. The Measurement Instrumentation and Sensors Handbook. CRC Press. ISBN 0-8493-8347-1. 1999. EPEL RM 53.08(023) M463.

5. Responsibility notice

The author(s) is (are) the only responsible for the printed material included in this paper